Baryonic matter and the medium modification of the baryon masses

Nam-Yong Ghim,[1,*] Ghil-Seok Yang,[2,†] Hyun-Chul Kim,[1,3,‡] and Ulugbek Yakhshiev[1,4,§]
[1]*Department of Physics, Inha University, Incheon 22212, Republic of Korea*
[2]*Department of General Education for Human Creativity, Hoseo University, Asan 31499, Republic of Korea*
[3]*School of Physics, Korea Institute for Advanced Study (KIAS), Seoul 02455, Korea*
[4]*Theoretical Physics Department, National University of Uzbekistan, Tashkent 100174, Uzbekistan*

(Received 10 February 2021; revised 29 April 2021; accepted 26 May 2021; published 7 June 2021)

We investigate the properties of baryonic matter within the framework of the in-medium modified chiral soliton model by taking into account the effects of surrounding baryonic environment on the properties of in-medium baryons. The internal parameters of the model are determined based on nuclear phenomenology at nonstrange sector and fitted by reproducing nuclear matter properties near the saturation point. We discuss the equations of state in different nuclear environments such as symmetric nuclear matter, neutron, and strange matters. We show that the results for the equations of state are in good agreement with the phenomenology of nuclear matter. We also discuss how the SU(3) baryons masses undergo changes in these various types of nuclear matter.

DOI: 10.1103/PhysRevC.103.064306

I. INTRODUCTION

It is of paramount importance to understand how the masses of hadrons undergo changes in nuclear medium, since it is deeply rooted in the restoration of chiral symmetry and even the quark confinement in quantum chromodynamics (QCD) [1–4]. As discussed in Ref. [1], the chiral condensate is known to be modified in nuclear matter, which reveals the mechanism as to how the spontaneous broken chiral symmetry is restored as the nuclear density increases. This also implies the changes of hadron masses in it, since the dynamical quark mass arises as a consequence of the spontaneous breakdown of chiral symmetry. Thus, understanding the medium modification of the nucleon mass has been one of the most significant issues well over decades [5]. Experimental data also indicate that the nucleon is modified in nuclei [6–11]. This means that other baryons may also undergo changes in nuclear medium [12–18]. When one considers the medium modification of baryons, one should keep in mind that nuclear matter itself is also affected self-consistently by the changes of baryons. However, it is very difficult to relate the medium modification of baryons to nuclear medium consistently, even in the isolated case of normal nuclear matter.

In the present work, we investigate the medium modification of the low-lying SU(3) baryons in symmetric matter, asymmetric matter, neutron matter, and strange baryonic matter consistently, based on a pion mean-field approach [19]. The general idea is based on the seminal paper by Witten [20,21]. In the large N_c (the number of colors) limit, the nucleon can be viewed as a state of N_c valence quarks bound by the meson mean fields that is produced self-consistently by the presence of the N_c valence quarks, since the mesonic quantum fluctuations are suppressed by the $1/N_c$ factor. This approach has been successfully applied for describing the various properties of both light and singly heavy baryons in a unifying manner [22–31]. The main idea of the pion mean-field approach is not to compute dynamical parameters within the chiral quark-soliton model [19,32], which realizes the pion mean-field approach explicitly, but to fix all relevant dynamical parameters by using the experimental data. For example, the masses of the baryon decuplet can be predicted by using the experimental data on those of the baryon octet and the mass of the Ω baryon [23]. Actually, this method was already used in the Skyrme model long time ago [33].

The pion mean-field approach can be also extended to the description of light and singly heavy baryons in nuclear medium. However, since the model is based on the quark degrees of freedom, one should consider the quark chemical potential [34], which means that it is rather difficult to connect the results from this approach directly to the properties of the baryons in nuclear matter. Thus, we will follow a variational approach that was adopted in the medium modified Skyrme models [35,36]. In these modified Skyrme models various properties of the nucleon and Δ isobar have been described in nuclear matter [36–39], and in finite nuclei [40–42]. The model enables one also to investigate nuclear matter properties [43–45].

Thus, we will show in this work how the pion mean-field approach can be extended to the investigation of the SU(3) baryon properties in both nuclear and strange baryonic environments. This can be achieved by introducing the density-dependent functionals as variational parameters. The

*Namyong.ghim@inha.ac.kr
†ghsyang@hoseo.edu
‡hchkim@inha.ac.kr
§yakhshiev@inha.ac.kr

density functionals will be parametrized and fitted completely in the SU(2) sector by taking into account available experimental and empirical data, the linear-response approximation being emphasized. This enables us to describe the strange baryonic matter and properties of baryons in different media (isospin symmetric, asymmetric, and strange baryonic matter).

The present paper is organized as follows. In Sec. II, we briefly review the pion mean-field approach, discussing the collective Hamiltonian and SU(3) baryon states in free space. Then we will proceed to consider a possible modification of the model to take into account the influence of the surrounding baryon environment on the properties of a single baryon in medium. In Sec. III, we discuss the results for the binding energy in symmetric matter and determine the variational parameters. The discussion of the properties of baryons in nuclear and strange nuclear matter will be followed in Sec. IV. We will also show how to fit the remaining part of the parameters. Then, we are able to discuss the properties of an arbitrary baryonic matter and the numerical results for the medium modifications of SU(3) baryons. Section V is devoted to the summary and conclusion of the present work and will give an outlook for future investigations. Some details of the model are compiled in the Appendix.

II. GENERAL FORMALISM

In the pion mean-field approach, the dynamics of the valence and sea quarks generates the chiral-quark soliton with hedgehog symmetry [21,46–48]. Hedgehog symmetry can be regarded as the minimal generalization of spherical symmetry, which can keep the pion mean fields effectively [48]. We are able to derive the effective collective Hamiltonian by considering the zero-mode quantization with hedgehog symmetry, taking into account the rotational $1/N_c$ corrections and the strange current-quark corrections from the explicit breaking of flavor SU(3) symmetry. Note that in the present approach the presence of N_c valence quarks constrains the right hypercharge $Y' = N_c/3$, which picks up safely the lowest allowed representations such as the baryon octet (**8**) and decuplet (**10**). However, Y' is constrained by the Wess-Zumino-Witten term in the SU(3) Skyrme model [49–51]. In this section, we will directly start from the collective Hamiltonian. For a detailed derivation, we refer to Ref. [52] (see also a review in Ref. [32]).

A. Pion mean-field approach

A pion mean-field approach, which is also called the chiral quark-soliton model, is based on the effective chiral action

$$S_{\rm eff} = -N_c {\rm Sp}\ln(i\partial\!\!\!/ + iMU^{\gamma_5} + i\hat{m}), \tag{1}$$

where Sp represents the functional trace over the four-dimensional Euclidean, spin, and flavor spaces. M stands for the dynamical quark mass that arises from the spontaneous breakdown of chiral symmetry. $\hat{m}$ designates the mass matrix of the current quarks $\hat{m} = {\rm diag}(m_{\rm u}, m_{\rm d}, m_{\rm s})$. We often write the mass matrix of the quarks in terms of the unity and Gell-mann matrices

$$\hat{m} = m_0\mathbf{1} + m_3\lambda_3 + m_8\lambda_8, \tag{2}$$

where

$$\begin{aligned} m_0 &= \frac{m_{\rm u} + m_{\rm d} + m_{\rm s}}{3}, \\ m_3 &= \frac{m_{\rm u} - m_{\rm d}}{2}, \\ m_8 &= \frac{m_{\rm u} + m_{\rm d} - 2m_{\rm s}}{2\sqrt{3}}. \end{aligned} \tag{3}$$

Since we consider the isospin asymmetry in the present work, we need to include m_3. We will treat $\hat{m}$ as a perturbation to the first order. The U^{γ_5} denotes the chiral field that is defined by

$$U^{\gamma_5}(\boldsymbol{r}) = \exp[i\pi^a\lambda^a\gamma_5] = \frac{1+\gamma_5}{2}U + \frac{1-\gamma_5}{2}U^\dagger. \tag{4}$$

The pseudo-Goldstone field $\pi^a(\boldsymbol{r})$ has flavor indices $a = 1, \cdots N_f^2 - 1$. Since we consider here the flavor SU(3) symmetry, we have $N_f = 3$. In flavor SU(2) symmetry ($N_f = 2$), the three components of the pion field are coupled with the axes of the three-dimensional Euclidean space. This is often called the hedgehog ansatz and is also called hedgehog symmetry [21,46–48]. Thus, the pion field in SU(2) is expressed as

$$\pi^a(\boldsymbol{r}) = n^a P(r), \quad n^a = \frac{x^a}{r}, \tag{5}$$

with $r = |\boldsymbol{x}|$. $P(r)$ is called the profile function for the soliton. In SU(3), we keep this hedgehog ansatz by the trivial embedding [21], so that the U field is expressed as

$$U(\boldsymbol{x}) = \exp(i\pi^a\lambda^a) = \begin{pmatrix} \exp[i(\boldsymbol{n}\cdot\boldsymbol{\tau}P(r)] & 0 \\ 0 & 1 \end{pmatrix}. \tag{6}$$

In fact, the symmetry of hedgehog ansatz imposes properly certain restrictions on the sytmmetry of the SU(3) soliton such that the spectrum of SU(3) baryons is correctly described [32,51,52]. $P(r)$ is called the profile function of the chiral soliton.

In the present pion mean-field approach, a baryon is viewed as a state consisting of the N_c valence quarks bound by the pion mean fields. This mean fields are created by the presence of the N_c valence quarks and interact with them self-consistently. Computing the baryonic correlation function in the large Euclidean time, we can derive the classical mass of the baryon. In fact, this mass is given as a functional of the chiral field. By minimizing this functional with respect to the profile function, we derive the equation of motion. We can solve it in a self-consistent manner, which can be found in Ref. [32] for technical details, we obtain the minimized classical mass and the profile function $P(r)$. The $U_{\rm cl}(\boldsymbol{x})$ with $P(r)$ is called the chiral soliton or the hedgehog soliton. However, since we take in the present work a "model-independent approach", we will not carry out the self-consistent calculation in the model. We will rather fix all the dynamical parameters by using the physical spectrum of the low-lying SU(3) baryons.

The mean-field solution or the classical solution $U_{\rm cl}(\boldsymbol{x})$ corresponds to the minimized classical nucleon that is required

to be quantized. $U_{\rm cl}(\boldsymbol{x})$ is not invariant under translation and rotation. This means that the soliton does not have proper quantum numbers to be a physical baryon. Thus, we perform the semiclassical quantization for the chiral soliton. We rotate $U_{\rm cl}(\boldsymbol{x})$ both in usual three-dimensional and flavor spaces in such a way that the classical mass remains unchanged. This is also called the zero-mode quantization. The axes of the three-dimensional space undergo the transformation as

$$x_i \to O_{ij}x_j. \tag{7}$$

This orthogonal matrix O_{ij} can be represented in terms of the SU(2) matrix S and Pauli matrices

$$O_{ij} = \tfrac{1}{2}\mathrm{Tr}(S\tau_i S^\dagger \tau_j). \tag{8}$$

Then $U_{cl}(\boldsymbol{x})$ is transformed as

$$\exp[i(\boldsymbol{n}'\cdot\boldsymbol{\tau})P(r)] = S\exp[i(\boldsymbol{n}\cdot\boldsymbol{\tau})P(r)]S^\dagger. \tag{9}$$

This leads to the expression for the transformed $U_{\rm cl}$ both in usual three-dimensional and flavor spaces,

$$RU_{\rm cl}(O\boldsymbol{x})R^\dagger = R\begin{pmatrix} Se^{i(\boldsymbol{n}\cdot\boldsymbol{\tau})P(r)}S^\dagger & 0 \\ 0 & 1\end{pmatrix}R^\dagger, \tag{10}$$

where R is the matrix in SU(3) flavor space. Note that there are seven zero modes in flavor SU(3) case, since the rotation with λ^8 commutes with $Se^{i(\boldsymbol{n}\cdot\boldsymbol{\tau})P(r)}S^\dagger$. In fact, this gives a constraint on the quantization, so that the right hypercharge Y_R is constrained to be

$$Y_R = -\frac{N_c}{3} \tag{11}$$

by the N_c valence quarks. In the Skyrme model, this is constrained by the Wess-Zumino term. This procedure of the zero-mode quantization yields the collective Hamiltonian, which we will discuss in the next subsection.

B. Collective Hamiltonian and Baryon states

If we consider both the explicit breakdowns of flavor SU(3) symmetry and isospin symmetry, we have four different contributions to the collective Hamiltonian, given as follows:

$$H = M_{\rm cl} + H_{\rm rot} + H_{\rm sb} + H_{\rm em}, \tag{12}$$

where $M_{\rm cl}$, $H_{\rm rot}$, and $H_{\rm sb}$ denote, respectively, the classical soliton mass, the $1/N_c$ rotational and symmetry-breaking corrections including the effects of isospin and flavor $\mathrm{SU(3)_f}$ symmetry breakings [23,53]. The last term $H_{\rm em}$ stands for the term arising from the isospin symmetry breaking caused by the electromagnetic self-energies [22]. We can neglect the modification of the electromagnetic self-energies in nuclear matter [42]. The classical energy arises from the N_c valence quarks in the pion mean fields and the sea quarks coming from the vacuum polarization in the presence of the N_c valence quarks: $E_{\rm cl} = N_c E_{\rm val} + E_{\rm sea}$. By minimizing $E_{\rm cl}$ with respect to the pion fields, we get the pion mean-field solution self-consistently, which yields the classical soliton mass $M_{\rm cl}$.

The rotational $1/N_c$ corrections, i.e., $H_{\rm rot}$, can be derived by the zero-mode collective quantization, since the zero modes are not at all small, one should take into account them completely. Regarding the angular velocities of the chiral soliton as small parameters, we can expand the quark propagator perturbatively in terms of the angular velocities, we find the rotational $1/N_c$ term $H_{\rm rot}$ as

$$H_{\rm rot} = \frac{1}{2I_1}\sum_{i=1}^{3}\hat{J}_i^2 + \frac{1}{2I_2}\sum_{p=4}^{7}\hat{J}_p^2. \tag{13}$$

This Hamiltonian depends on two moments of inertia $I_{1,2}$ and expressed in terms of the operators $\hat{J}_i$ corresponding to the generators of the SU(3) group. I_1 and I_2 give the splitting between different representations of the SU(3) group. The symmetry breaking part of the Hamiltonian has the following form:

$$\begin{aligned} H_{\rm sb} &= (m_{\rm d}-m_{\rm u})\left(\frac{\sqrt{3}}{2}\alpha D_{38}^{(8)}(\mathcal{A}) + \beta\hat{T}_3 + \frac{1}{2}\gamma\sum_{i=1}^{3}D_{3i}^{(8)}(\mathcal{A})\hat{J}_i\right) \\ &+ (m_{\rm s}-\bar{m})\left(\alpha D_{88}^{(8)}(\mathcal{A}) + \beta\hat{Y} + \frac{1}{\sqrt{3}}\gamma\sum_{i=1}^{3}D_{8i}^{(8)}(\mathcal{A})\hat{J}_i\right), \end{aligned} \tag{14}$$

where α, β, and γ depend on the moments of inertia that are expressed as

$$\begin{aligned} \alpha &= -\left(\frac{2}{3}\frac{\Sigma_{\pi N}}{m_{\rm u}+m_{\rm d}} - \frac{K_2}{I_2}\right), \\ \beta &= -\frac{K_2}{I_2}, \quad \gamma = 2\left(\frac{K_1}{I_1} - \frac{K_2}{I_2}\right). \end{aligned} \tag{15}$$

Here $K_{1,2}$ represent the anomalous moments of inertia of the soliton. $m_{\rm u}$, $m_{\rm d}$, and $m_{\rm s}$ denote the current-quark masses of the up, down, and strange quarks, respectively. The $\bar{m}$ designates the average current-quark mass of the up and down quarks. The $D_{ab}^{(\mathcal{R})}(\mathcal{A})$ indicate the SU(3) Wigner D functions in the representation $\mathcal{R}$. The $\hat{Y}$ and $\hat{T}_3$ are the operators of the hypercharge and the third component of the isospin, respectively.

In the representation $(p,\ q)$ of the SU(3) group, the sum of the generators can be expressed in terms of p and q,

$$\sum_{i=1}^{8}J_i^2 = \frac{1}{3}[p^2 + q^2 + p\,q + 3(p+q)], \tag{16}$$

which yields the eigenvalues of the rotational collective Hamiltonian $H_{\rm rot}$ in Eq. (15) as follows:

$$\begin{aligned} E_{(p,\,q),\,J} &= \frac{1}{2}\left(\frac{1}{I_1} - \frac{1}{I_2}\right)J(J+1) - \frac{3}{8I_2} \\ &+ \frac{1}{6I_2}[p^2 + q^2 + 3(p+q) + p\,q]. \end{aligned} \tag{17}$$

A corresponding eigenfunction is called the collective wave function for a SU(3) baryon with the quantum numbers of flavor $\mathcal{F} = (Y, T, T_3)$ and spin $\mathcal{S} = (Y', J, J_3)$,

$$\psi_{_B}^{(\mathcal{R})}(\mathcal{A}) = \sqrt{\dim(\mathcal{R})}(-1)^{J_3+Y'/2}D_{\mathcal{F}\mathcal{S}}^{(\mathcal{R})*}(\mathcal{A}), \tag{18}$$

where $D_{\mathcal{F}\mathcal{S}}^{(\mathcal{R})*}$ are again the Wigner D functions in a representation $\mathcal{R}$ and $\dim(\mathcal{R})$ designates the corresponding dimension of the representation $\mathcal{R}$.

Knowing the eigenvalues and eigenfunctions of the SU(3) baryon states, we can get their masses of which the explicit forms are presented in the Appendix. For a detailed formalism relating to the collective Hamiltonian and baryon states, we refer the reader to Ref. [23], where all dynamical parameters such as I_1, I_2, K_1, K_2, α, β, and γ are determined by using the experimental data in a "*model-independent way*," so that we can avoid a specific dynamics of the chiral soliton models. We now turn to how the model can be extended to nuclear medium.

C. Solitons in nuclear matter

Since we have determined all the dynamical parameters by incorporating experimental information, we will follow the same strategy also in nuclear matter. We will fix the density-dependent variational parameters by using the experimental and empirical data on the properties of nuclear matter. So, we start from the average energy E^* per baryon in a baryonic system[1]

$$\frac{E^*}{A} = \frac{ZM_p^* + NM_n^* + \sum_{s=1}^{3} N_s M_s^*}{A}, \tag{19}$$

where Z and N are the numbers of protons and neutrons, respectively, and N_s is the corresponding number of the strange baryons with the corresponding strangeness S, $s = |S|$. A stands for the total number of the baryons $A = Z + N + N_1 + N_2 + N_3$. Having carried out a simple manipulation, we can rewrite E^*/A as

$$\frac{E^*}{A} = M_N^* \left(1 - \sum_{s=1}^{3} \delta_s\right) + \frac{1}{2}\delta M_{np}^* + \sum_{s=1}^{3} \delta_s M_s^*, \tag{20}$$

where $M_N^* = (M_p^* + M_n^*)/2$ denotes the average mass of nucleons, $M_{np}^* = M_n^* - M_p^*$ designates the mass difference of the neutron and the proton in medium. In addition, we introduce the parameter for isospin asymmetry $\delta = (N - Z)/A$. $\delta_s = N_s/A$ represents the parameter for the strangeness fraction with the corresponding value of subscript s. We can take $s = 1$, 2, or 3, depending on the hyperons with strangeness S we put.

The binding energy per baryon in a baryonic matter can be defined as the difference of the medium average energy per baryon E^*/A and the energy per baryon E/A for the noninteracting baryonic system. If one takes the number of the baryons to be infinity, which we can call it the infinite baryon-matter approximation, then we express the binding energy per baryon in terms of the following external parameters: a normalized baryonic density $\lambda = \rho/\rho_0$, the isospin asymmetry parameter δ, and the strangeness fraction parameter δ_s with given s. Consequently, the binding energy is then written as

$$\begin{aligned}\varepsilon(\lambda, \delta, \delta_1, \delta_2, \delta_3) &= \frac{E^*(\lambda, \delta, \delta_1, \delta_2, \delta_3) - E}{A} \\ &= \Delta M_N(\lambda, \delta, \delta_1, \delta_2, \delta_3)\left(1 - \sum_{s=1}^{3} \delta_s\right) \\ &\quad + \frac{1}{2}\delta\, \Delta M_{np}(\lambda, \delta, \delta_1, \delta_2, \delta_3) \\ &\quad + \sum_{s=1}^{3} \delta_s \Delta M_s(\lambda, \delta, \delta_1, \delta_2, \delta_3),\end{aligned} \tag{21}$$

where $\Delta M_N = M_N^* - M_N$ denotes the isoscalar mass change, whereas $\Delta M_{np} = M_{np}^* - M_{np}$ stands for the neutron-proton mass change in nuclear medium. They are explicitly expressed in terms of the in-medium modified functionals of the chiral soliton

$$\begin{aligned}\Delta M_N &= M_{\rm cl}^* - M_{\rm cl} + E_{(1,1)1/2}^* - E_{(1,1)1/2} \\ &\quad - D_1^* - D_2^* + D_1 + D_2,\end{aligned} \tag{22}$$

$$\Delta M_{np} = d_1^* - d_2^* - d_1 + d_2, \tag{23}$$

where the explicit expressions for $D_{1,2}$ and $d_{1,2}$ in free space are given in the Appendix [see Eqs. (A9)–(A12)]. $D_{1,2}$ represent the linear m_s corrections of flavor SU(3) symmetry breaking whereas $d_{1,2}$ denote the effects of isospin symmetry breaking. They are related to the model functionals to be discussed below through α, β, and γ defined in Eq. (15). Note that for the mass differences of the hyperons $\Delta M_s = M_s^* - M_s$ ($s = 1, 2, 3$) we have the different expressions for the baryon octet and decuplet. For the moment, let us concentrate on the strange baryonic medium made of the hyperons in the baryon octet as in the case of the nonstrange baryons. Thus, we adopt the following expressions for ΔM_s:

$$\begin{aligned}\Delta M_1 &= \frac{M_\Lambda^* + M_\Sigma^*}{2} - \frac{M_\Lambda + M_\Sigma}{2} \\ &= M_{\rm cl}^* - M_{cl} + E_{(1,1)1/2}^* - E_{(1,1)1/2},\end{aligned} \tag{24}$$

$$\begin{aligned}\Delta M_2 &= M_\Xi^* - M_\Xi \\ &= M_{\rm cl}^* - M_{cl} + E_{(1,1)1/2}^* - E_{(1,1)1/2} + D_2^* - D_2,\end{aligned} \tag{25}$$

$$\Delta M_3 = 0. \tag{26}$$

We now discuss how we can modify the dynamical parameters of the pion mean-field approach in nuclear medium. We follow the strategy presented in Refs. [44,45] and assume that the dynamical parameters discussed in Subsection II B, i.e., $M_{\rm cl}$, $I_{1,2}$ and $K_{1,2}/I_{1,2}$, will be modified as follows:

$$M_{\rm cl} \to M_{\rm cl}^* = M_{\rm cl} f_{\rm cl}(\lambda, \delta, \delta_1, \delta_2, \delta_3), \tag{27}$$

$$I_1 \to I_1^* = I_1 f_1(\lambda, \delta, \delta_1, \delta_2, \delta_3), \tag{28}$$

$$I_2 \to I_2^* = I_2 f_2(\lambda, \delta, \delta_1, \delta_2, \delta_3), \tag{29}$$

$$\begin{aligned}(m_{\rm d} - m_{\rm u})\frac{K_{1,2}}{I_{1,2}} &\to E_{\rm iso}^* \\ &= (m_{\rm d} - m_{\rm u})\frac{K_{1,2}}{I_{1,2}} f_0(\lambda, \delta, \delta_1, \delta_2, \delta_3),\end{aligned} \tag{30}$$

[1]Asterisks "$*$" in the superscripts denote in-medium modified quantities.

$$(m_s - \bar{m})\frac{K_{1,2}}{I_{1,2}} \to E^*_{\rm str} = (m_s - \bar{m})\frac{K_{1,2}}{I_{1,2}} f_s(\lambda, \delta, \delta_1, \delta_2, \delta_3), \quad (31)$$

where $f_{\rm cl}$, $f_{0,1,2}$, and f_s represent the functions of nuclear densities for nuclear medium. We will parametrize them based on information about nuclear matter in the next section. One should keep in mind that in general one can consider density dependencies in a different manner, depending on the isospin splitting and the mass splittings in different representations [see Eqs. (30) and (31)]. As mentioned previously, we assume that the electromagnetic corrections to the neutron-proton mass difference is only weakly affected by nuclear medium. So, we will not consider them in the present work. We ignore also the effects of isospin symmetry breaking coming from baryons on the binding energy except for the nucleons, assuming the small strangeness fraction up to normal nuclear matter densities.

III. NUCLEAR PHENOMENOLOGY

In the present section, we will discuss the results related to symmetric nuclear matter, isospin asymmetric nuclear matter, and more general baryonic matter, one by one. We first start with ordinary symmetric nuclear matter.

A. Symmetric nuclear matter

We first consider isospin symmetric and nonstrange ordinary nuclear matter with the external parameters $\delta = 0$ and $\delta_s = 0$. Then we can parametrize the density functions such as $f_{\rm cl}$, f_1 and f_2. In consequence, we are able to determine the values of the corresponding parameters phenomenologically. For example, they are related to the properties of isospin-symmetric nuclear matter near the saturation point, i.e., at the normal nuclear matter density $\rho_0 \sim (0.16\text{–}0.17)\,\mathrm{fm}^{-3}$. We remind that in the case of isospin-symmetric nuclear matter the binding energy per unit volume is given by

$$\mathcal{E} \equiv \varepsilon_V(\rho)\frac{A}{V} = \rho_0 \lambda\, \varepsilon_V(\lambda). \quad (32)$$

Following the ideas presented in Refs. [44,45], we choose the parametrization of the three medium functions $f_{\rm cl}$, f_1, and f_2, which are independent of the asymmetry parameter δ and the strangeness fraction parameters δ_s. Furthermore, we will parametrize them for simplicity in a linear density-dependent form

$$f_{\rm cl}(\lambda) = (1 + C_{\rm cl}\lambda), \quad f_{1,2}(\lambda) = (1 + C_{1,2}\lambda). \quad (33)$$

It is enough to employ this linear-density approximation, since the equations of state (EoS) for nuclear matter are well explained. However, if the density of nuclear matter becomes larger than the normal nuclear matter density, then one may need to consider higher-order corrections to the parametrization we use. Nevertheless, we will compute the baryon properties as functions of the nuclear matter density up to $3\rho_0$ to see how far the linear-density approximation works well.

The properties of symmetric nuclear matter near the saturation point can be related to the isoscalar nucleon mass change in the nuclear medium

$$\varepsilon_V(\lambda) = \epsilon(\lambda, 0, 0, 0, 0) = \Delta M_N(\lambda). \quad (34)$$

This implies that α, β, and γ will not be changed in symmetric nuclear medium. We will see that they will come into play when we consider asymmetric nuclear and strange baryonic matter. Then we can easily obtain the following formula for the density dependence of the volume energy

$$\varepsilon_V(\lambda) = \mathcal{M}_{\rm cl} C_{\rm cl}\lambda - \frac{3C_1\lambda}{8I_1(1 + C_1\lambda)} - \frac{3C_2\lambda}{4I_2(1 + C_2\lambda)}. \quad (35)$$

We now proceed to calculate the properties of nuclear matter near the saturation point $\lambda = 1$ by expanding the volume energy with respect to the nuclear density. The expansion coefficients have clear physical meanings related to the properties of nuclear matter at the saturation point. They are given as follows:

$$a_V = \varepsilon_V(1), \quad P_0 = \rho_0 \lambda^2 \frac{\partial \varepsilon_V(\lambda)}{\partial \lambda}\bigg|_{\lambda=1}, \quad K_0 = 9\lambda^2 \frac{\partial^2 \varepsilon_V(\lambda)}{\partial \lambda^2}\bigg|_{\lambda=1}, \quad (36)$$

where a_V denotes the value of the volume energy, P_0 stands for that of the pressure, and K_0 represents the compressibility of nuclear matter at the saturation point. The value of the coefficient of the volume term a_V is well known from the analysis of atomic nuclei according to the semi-empirical Bethe-Weizsäker formula [54,55]. So, we choose the well-known value $a_V = -16$ MeV. The stability of nuclear matter requires the zero value of the pressure $P_0 = 0$ at the saturation point. The compressibility of nuclear matter within various approaches is found to be $K_0 \sim (290 \pm 70)$ MeV [56–61]. Based on a comprehensive reanalysis of recent data on the energies of the giant monopole resonance (GMR) in even-even $^{112-124}$Sn and $^{106,100-116}$Cd and earlier data on $58 \leqslant A \leqslant 208$ nuclei in Ref. [62], the value of the compressibility can be taken to be $K_0 \sim (240 \pm 20)$ MeV [63]. Following this analysis, we choose $K_0 = 240$ MeV in the present work. Thus, the three parameters in the density functions given in Eq. (33) can be fitted to be

$$C_{\rm cl} = -0.0561, \quad C_1 = 0.6434, \quad C_2 = -0.1218. \quad (37)$$

Now we can predict the skewness of symmetric nuclear matter, which is defined from the fourth coefficient in the series of the volume energy:

$$Q = 27\lambda^3 \frac{\partial^3 \varepsilon_V(\lambda)}{\partial \lambda^3}\bigg|_{\lambda=1} = -\frac{117}{2}\left(\frac{C_1^3}{(1 + C_1)^4 I_1} - \frac{2C_2^3}{(1 + C_2)^4 I_2}\right) = -182\ \text{MeV}. \quad (38)$$

The result is consistent with those from other model calculations. For example, one can find similar results from the Hartree-Fock approach based on the Skyrme interactions [64] and the isospin- and momentum-dependent interaction (MDI)

model [65]. We want to emphasize that these coefficients in the expansion of the volume energy can be used for understanding the properties of symmetric nuclear matter.

B. Asymmetric nuclear matter

Since the asymmetric nuclear matter arises from the isospin symmetry breaking, Eq. (45) plays the key role in describing the asymmetric nuclear matter. Following the strategy taken from Refs. [44,45], we find that the density function f_0 can be defined as a function of the normalized density λ and isospin asymmetry parameter δ in the following form:

$$f_0(\lambda,\delta) = 1 + \frac{C_{\rm num}\lambda\,\delta}{1 + C_{\rm den}\lambda}, \tag{39}$$

where $C_{\rm num}$ and $C_{\rm den}$ can be determined phenomenologically. This parametrization is also chosen under the simple assumption: that is, if δ is zero or ρ is zero, then the value of f_0 is equal to 1. Moreover, using the parametrized form given in Eq. (39), one can see that various properties of asymmetric nuclear matter are well described, e.g., the binding energy of asymmetric nuclear matter will be given as a quadratic form with respect to the asymmetry parameter δ.[2]

The nuclear symmetry energy is defined as the second derivative of the binding energy with respect to δ:

$$\varepsilon_{\rm sym}(\lambda) = \frac{1}{2!}\frac{\partial^2\varepsilon(\lambda,\delta,0,0,0)}{\partial\delta^2}\bigg|_{\delta=0}. \tag{40}$$

As in the case of the volume energy, we can expand $\varepsilon_{\rm sym}$ around the saturation point $\lambda = 1$ as follows:

$$\varepsilon_{\rm sym}(\lambda) = a_{\rm sym} + \frac{L_{\rm sym}}{3}(\lambda-1) + K_{\rm sym}\frac{(\lambda-1)^2}{18} + \cdots, \tag{41}$$

from which we obtain the value of the nuclear symmetry energy at saturation point $a_{\rm sym}$, that of its slope parameter $L_{\rm sym}$, and the asymmetric part of the compressibility $K_{\rm sym}$. They are explicitly written as

$$a_{\rm sym} = -\frac{9}{20}\frac{C_{\rm num}(b-7r/18)}{(1+C_{\rm den})}, \tag{42}$$

$$L_{\rm sym} = -\frac{27}{20}\frac{C_{\rm num}(b-7r/18)}{(1+C_{\rm den})^2}, \tag{43}$$

$$K_{\rm sym} = \frac{81C_{\rm den}C_{\rm num}(b-7r/18)}{10(1+C_{\rm den})^3}, \tag{44}$$

where $b = (m_{\rm d} - m_{\rm u})\beta$ and $r = (m_{\rm d} - m_{\rm u})\gamma$.

The value of the nuclear symmetry energy at the saturation point is known to be in the range $\varepsilon_{\rm sym}(1) \sim 30{-}34$ MeV. So, we can take the average value $a_{\rm sym} = 32$ MeV. The correlation between the value of the symmetry energy at the saturation density and that of its slop parameter taken from the neutron skip thickness experiments of ^{68}Ni, ^{120}Sn, and ^{208}Pb indicates the tendency that heavier the nucleus yields larger the value of $L_{\rm sym}$, which corresponds to that of $a_{\rm sym}$ [66]. As a result, one can choose $L_{\rm sym} = 60$ MeV for the asymmetric nuclear matter. We mainly use these values of $a_{\rm sym}$ and $L_{\rm sym}$ in the course of the present calculation, if it is not specified otherwise.[3] The empirical values of these two quantities will adjust those of $C_{\rm num}$ and $C_{\rm den}$, respectively. To check the stability of the present results for to neutron matter ($\delta = 1$), however, we have analyzed the different choices for the $a_{\rm sym}$ and $L_{\rm sym}$ with small variations. Note that the results are very insensitive to $a_{\rm sym}$ in the range of its values discussed above. Thus, we will only show the variations of $L_{\rm sym}$ and the possible two choices of $L_{\rm sym}$ in this work are listed in Table I. All the parameters are actually fitted in this way in relation to nuclear matter properties at the saturation density, so the present model can be regarded as a simple model of nuclear matter with five parameters. Using the values of the parameters for the symmetry energy listed in Table I, we are able to discuss the EoS for asymmetric nuclear matter, extrapolating to the low and high density regions, and to predict various properties of nuclear matter. In particular, employing Set I, we can calculate the third coefficient in the expansion of the symmetry energy, which leads to $K_{\rm sym} = -135$ MeV. The following quantities, which are related to $K_{\rm sym}$, can be also determined as

TABLE I. Possible sets of the parameters for the symmetry energy.

	$a_{\rm sym}$ [MeV]	$L_{\rm sym}$ [MeV]	$C_{\rm num}$	$C_{\rm den}$
Set I	32	60	65.60	0.60
Set II	32	50	78.72	0.92

$$K_\tau = K_{\rm sym} - 6L_{\rm sym} = -495\ \text{MeV},$$
$$K_{(0,2)} = K_\tau - \frac{Q}{K_0}L_s = -450\ \text{MeV}. \tag{45}$$

The calculated values of K_τ and $K_{0,2}$ are in good agreement with the results from other approaches. As an example, we can compare the range of $K_{0,2}$ value with that from the phenomenological momentum-independent model $-477\,\text{MeV} \leqslant K_{0,2} \leqslant -241\,\text{MeV}$ [67].

Figure 1 draws illustratively the density dependence of binding energy per nucleon, given the different values of the asymmetry parameter δ. We find that the results are rather stable to the change of values of the parameters $a_{\rm sym}$ and $L_{\rm sym}$. In particular, the present results change only slightly as the values of $L_{\rm sym}$ are varied from 50 to 60 MeV.

It is natural that the neutron matter gets less bound relatively to the symmetric matter, as already shown in Fig. 1. The density dependence of the binding energy per nucleon in symmetric matter and neutron matter are in agreement with those from other models and phenomenological ones. In particular, it is consistent with Akmal-Pandharipande-Ravenhall (APR) predictions [68] in the range of λ, where the simple linear-density approximation is justified for the medium modification of the corresponding soliton functionals in nuclear matter. As λ increases, the present EoS becomes stiffer such

[2]Note that there is another δ factor in Eq. (21).

[3]We will not use any other input data in the strangeness sector.

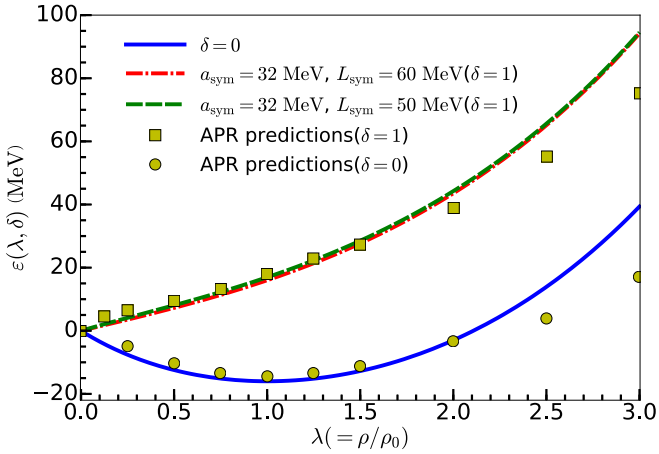

FIG. 1. Binding energy per nucleon $\varepsilon(\lambda, \delta) \equiv \varepsilon(\lambda, \delta, 0, 0, 0)$ as a function of the normalized nuclear matter density $\lambda = \rho/\rho_0$ in unit of MeV. The blue solid curve depicts the symmetric matter $\delta = 0$ whereas the red dot-dashed and green dashed curves illustrate those of neutron matter $\delta = 1$ for the possible two sets of symmetry energy parameters, respectively. The present results are compared with those given in APR predictions [68] that are given by the yellow circles and boxes, respectively.

that one can get the larger masses of neutron stars than the solar mass. However, as the density becomes higher than $\lambda = 2$, the linear density approximation may not be enough, which requires one to introduce higher-order nonlinear terms.

The nuclear symmetry energy plays a very important role in understanding the EoS of nuclear matter and, in particular, of the neutron matter. Figure 2 exhibits how the nuclear symmetry energy depends on λ. We present the results with the two sets of the parameters $a_{\rm sym}$ and $L_{\rm sym}$ listed in Table I. When the value of the slop parameter $L_{\rm sym}$ gets smaller, the

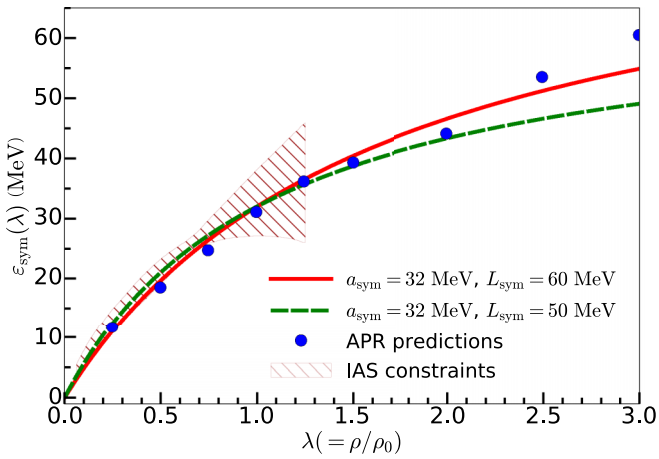

FIG. 2. Nuclear symmetry energy $\varepsilon_{\rm sym}(\lambda)$ as a function of the normalized nuclear density $\lambda = \rho/\rho_0$ in unit of MeV. The results with the possible two sets of parameters for the symmetry energy are represented by the red solid and green dashed curves, respectively. The results are compared with those from Ref. [68], which are marked by the blue circles and those from the IAS constraints [69] shown by the shaded region.

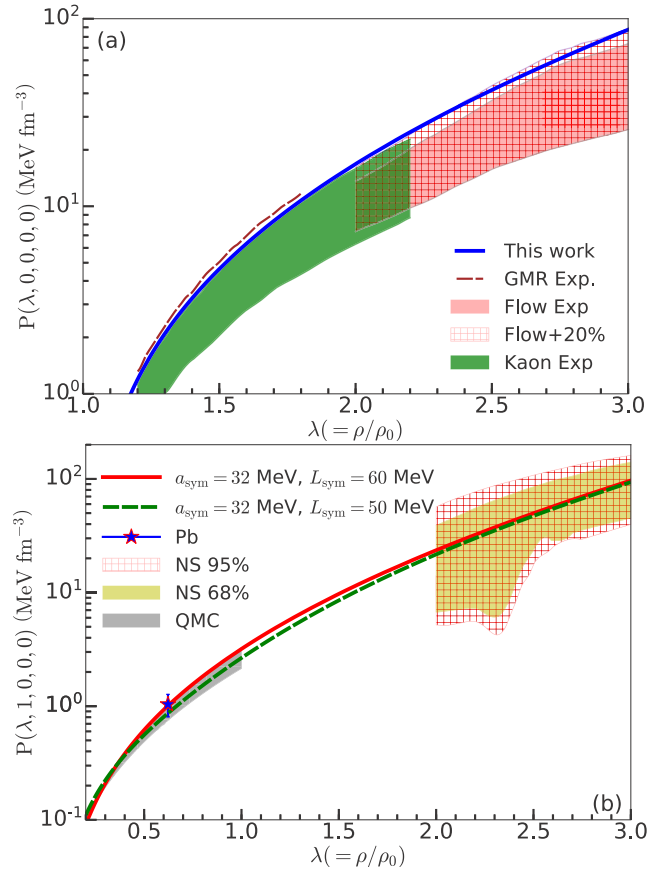

FIG. 3. Numerical results for the pressure $P(\lambda, \delta, 0, 0, 0)$. In panel (a), the results are drawn for the symmetric nuclear matter ($\delta = 0$), compared with the data taken from GMR [70,71], flow [72], flow+20% [73,74], and kaon [71,75] experiments, whereas in panel (b) those for the neutron matter ($\delta = 1$) are depicted, compared with the data from Pb experiment [76], NS 95% [73], NS 68% [73], and Quantum Monte Carlo calculations [76–78]. In the neutron matter, the present results are obtained for the two sets of the parameters: red solid and green dashed curves draw the results with Set I and Set II, respectively.

symmetry energy becomes slightly larger than that obtained by using the larger value of $L_{\rm sym}$ till the normal nuclear matter density ($\lambda = 1$), then it becomes smaller than that with $L_{\rm sym} = 60$ MeV. Note that, however, the present results are quite stable as the parameters vary, and are consistent with those obtained from other approaches and extracted data. In particular, the results are in good agreement with APR predictions till the density reaches $\lambda = 2$. At large nuclear matter densities the results of the symmetry energy become smaller than the values of the APR symmetry energy. The present results are also in good agreement with the bounded values of the symmetry energy, obtained from the analysis of isobaric states (IAS) [69], which is represented by the shaded region in Fig. 2.

For completeness, we present in Figs. 3(a) and 3(b) the density dependence of the pressure in the symmetric nuclear matter and and in the neutron matter, respectively. The present results for the pressure are in good agreement with those

obtained from other approaches and the extracted data, in particular, in the range of $\rho \in [0, 3\rho_0]$.

For example, in Fig. 3(a) the result of this work for the pressure $P(\lambda, 0, 0, 0, 0)$ in the symmetric matter ($\delta = 0$), which is drawn in the blue solid curve, is compared with the data extracted from various experiments. In particular, the present result is in good agreement with the data in the range of $1.2 \leqslant \lambda \leqslant 1.7$ extracted from the GMR experiments [70,71] for heavy nuclei, which are shown by the dashed curve. However, in Ref. [72] the flow experimental data on ^{197}Au nuclei collision are analyzed, which are illustrated by the red-shaded region and correspond to the zero-temperature equation of state for the symmetric nuclear matter. Additional studies are presented in Refs. [73,74], which were extended to the range of the validity taking into account the mass-radius relation of neutron stars from observational data. In Fig. 3(a) data in the extended region are denoted as "Flow + 20%." One can see that our equations of state are consistent with the newly predicted range. The EoS for the symmetric nuclear matter in the range of $1.2 \leqslant \lambda \leqslant 2.2$ can also be constrained by the kaon production data from high-energy nucleus-nucleus collision [71,75]. They are shown in the green-colored region. The present results lie also within that region and, in general, are consistent with all the data extracted from different methods.

In Fig. 3(b), the results for the pressure are presented in the neutron matter ($\delta = 1$). We again depict the results for $P(\lambda, 1, 0, 0, 0)$ with the two sets of the parameters $a_{\rm sym}$ and $L_{\rm sym}$. They are represented by the red solid and green dashed curves, respectively, in Fig. 3(b). One can see that EoS obtained in the present work are quite stable with the varying parameters that define the symmetric energy. We compare the results with those extracted from the several experiments. For example, the weighted average of the experimental data on the neutron skin thickness in ^{208}Pb is indicated by the red-colored star at subnuclear density [76]. The studies in Ref. [73] provide a constraint for the pressure values of neutron star matter from astrophysical observation data. In Fig. 3(b), this constraint is labeled as "NS 95%" and "NS 68%" for the two different confidence limits. There are also results at the low-density region from the quantum Monte Carlo calculation (QMC) [76–78]. They are denoted by the gray-shaded region. One can see that our results are in an excellent agreement with all extracted data in the different ways in all density regions presented in the figure.

In short summary, this simple five-parametric model for nuclear matter within the framework of the model-independent chiral soliton approach describes the isospin-symmetric and neutron matter properties very well. This implies that the meson mean-field approach quite successful not only for explaining various properties of light and singly-heavy baryons in free space [23] but also for describing phenomenologically nuclear matter properties, based on minimal phenomenological information in the nonstrange sector.

C. Baryonic matter

We now proceed to baryonic matter properties in a more general case taking into account also the strange baryons. So far, we have concentrated on the nonstrange sector and fitted our parameters according to the nuclear phenomenology in nonstrange sector. We have also parametrized the influence of surrounding nuclear matter to the in-medium nucleon properties in such a way that the binding energy per nucleon appears as a quadratic term in the isospin asymmetry parameter δ. Following the strategy used in the nonstrange sector we can parametrize the influence of baryonic matter with the strangeness content. In doing that, we will consider the simplicity as a guiding principle. Therefore, as a first step we will not introduce any new parameter and try to describe the strangeness-mixed baryonic matter. For that purpose, we expand the binding energy per baryon into the series in the region with the small values of the isospin-asymmetry parameter δ and strangeness-mixing parameters δ_s. Consequently, the series of the binding energy per nucleon at the small values of isospin asymmetry and hyperon mixture parameters δ and δ_s ($i = 1, 2, 3$) given in Eq. (31) can be written as

$$\begin{aligned}\varepsilon(\lambda, \delta, \delta_1, \dots) &= \varepsilon_V(\lambda) + \varepsilon_{\rm sym}(\lambda)\delta^2 \\ &+ \sum_{s=1}^{3} \frac{\partial\, \varepsilon(\lambda,\ \delta,\ \delta_1, \dots)}{\partial\, \delta_s}\bigg|_{\delta=\delta_1=\cdots=0} \delta_s \\ &+ \frac{1}{2}\sum_{s,p=1}^{3} \frac{\partial^2\, \varepsilon(\lambda,\ \delta,\ \delta_1, \dots)}{\partial\, \delta_s \partial \delta_p}\bigg|_{\delta=\delta_1=\cdots=0} \delta_s\delta_p \\ &+ \cdots, \end{aligned} \tag{46}$$

where, for convenience of discussion, the terms of the standard volume and symmetry energies for ordinary nuclear matter are explicitly separated as the first and the second ones. It is obvious that the linear terms in δ are absent due to the quadratic dependence of the binding energy per baryon on it.

Next, assuming that the contributions of higher-order terms in δ_s are negligible, we can choose f_s's similar to f_0 [see Eq. (39)] as a linear form in δ_s.[4] Furthermore, we parametrize f_s in such a way that there is no δ dependence. These parametrization will keep all our discussions in the nonstrange sector intact. Then we have the following forms of the remaining density functions

$$f_s(\lambda,\ \delta,\ \delta_1, \dots) = 1 + g_s(\lambda)\delta_s. \tag{47}$$

We also assume that the third term in Eq. (46) is equals to zero. This leads to the following form of g_s:

$$\begin{aligned} g_s(\lambda) &= s g(\lambda), \\ g(\lambda) &= -\frac{5(M^*_{\rm cl} - M_{cl} + E^*_{(1,1)1/2} - E_{(1,1)1/2})}{3(m_s - \hat{m})} \\ &\times \left(6\frac{K_2}{I_2} + \frac{K_1}{I_1}\right)^{-1}. \end{aligned} \tag{48}$$

This final expression is a reasonable one, because the strangeness content of nuclei is negligible and g_s at small densities in Eq. (48) maximizes the energy for $\delta_s = 0$. This choice is advantageous, since it allows one to fit all parameters

[4]Note that this is also the simplest choice.

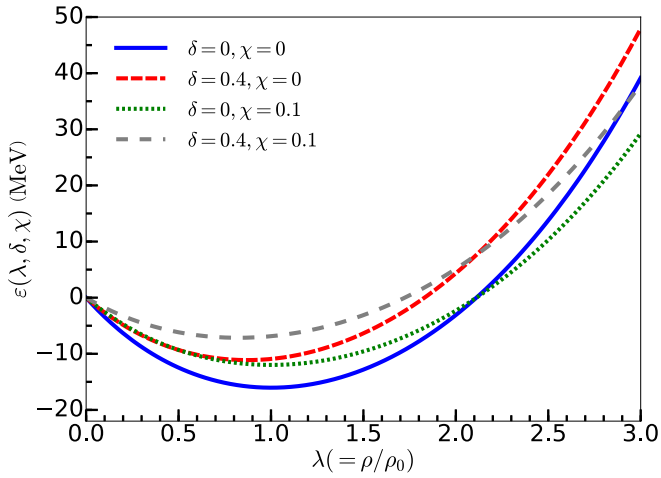

FIG. 4. Binding energy per nucleon $\varepsilon(\lambda, \delta, \chi)$ as a function of the normalized nuclear matter density $\lambda = \rho/\rho_0$. The results are drawn for the ordinary isospin symmetric matter in the blue solid curve, the strangeness mixed isospin-symmetric matter in the red dashed one, the pure neutron matter in the green dotted one and the strangeness-mixed isospin-asymmetric matter in the gray space-dashed one, respectively. The parameters of the symmetry energy are taken from Set I in Table I.

in the SU(2) sector. As a result, we have no internal density parameters in the SU(3) sector and we do not need to relate this approach to the strange matter phenomenology. All results in the strangeness sector can be considered as predictions in this simplified work.

In the medium-modified SU(3) sector, we have only one external free parameter, which is the fraction of strange matter. In order not to distinguish the species of strange matter, we introduce the strangeness-mixing parameter χ defining it as the following simple and reasonable way: $\delta_s = s\chi$. So, we can discuss the strangeness effects by considering nonzero values of the free parameter χ.

The strangeness effects due to the surrounding environment may come from the different combinations, e.g., the isospin-symmetric matter with the strangeness-mixing or the isopin-asymmetric matter with the strangeness mixing. The binding energies per nucleon for different nuclear matters are presented in Fig. 4, which shows clearly how the binding energy undergoes modification as the strangeness content varies together with δ changed. For comparison, we again depict the binding energy for symmetric matter in the blue solid curve, for the isospin-asymmetric matter in the red-dashed one, for the strangeness-mixed isospin-symmetric matter in the green-dotted curve and the strangeness-mixed isospin-asymmetric matter in the gray space-dashed curve, respectively. One can see that the strangeness mixing leads to the less bound system at subnuclear matter densities while the binding energy per nucleon varies rather slowly as λ increases, so that its magnitude becomes even larger than those in both isosymmetric and isoasymmetric nuclear matter at supranuclear matter densities, i.e., compare the blue solid curve and the green dotted one or the red dashed and grey dashed ones, respectively. At large densities the strange matter may be a more favorable system so that strange quark stars are allowed to exist with a smaller mass due to the softening EoS in comparison with neutron stars.

The present results are in line with those from an extended Brueckner-Hartree-Fock formalism [79]. Although their approach has a problem in reproducing the correct value of the binding energy per nucleon at normal nuclear matter density, the tendency of the strangeness fraction is very similar to the present one. They also found that strangeness mixing leads to the shallowing of the curve for the binding energy and negligible shifting to the higher density region. We also want to mention that the present results are consistent with those from other approaches and model calculations. For example, see a recent review [13] about theoretical approaches to the production of hyperons, baryon resonance and hyperon matter in heavy-ion collision (see also Ref. [80]). In particular, the dependence of the binding energy on nuclear matter density with the strangeness mixed was discussed in Ref. [13] and the results are qualitatively similar to the present ones. In Ref. [81] the G-matrix formalism was used with the Nijmegen soft-core baryon-baryon potentials plugged in. Since they consider the fraction of strangeness in terms of the Λ, Σ, and Ξ baryons, it is not easy to make a direct comparison with the present work. As the fraction of strangeness $(\Lambda + \Sigma)$ increases in Ref. [81], the magnitude of the binding energy gets larger until it reaches around $\chi_{\Lambda+\Sigma} \approx 0.3$. Then, it starts to decrease. This indicates that as the strangeness fraction increases by more than 30%, the tendency of the binding energy becomes similar to the present result drawn in Fig. 4. However, the results from Ref. [81] at higher densities behave differently, compared with the present ones. The results for the binding energy from Ref. [82], which employed the relativistic mean-field approximation with the Nijmegen soft-core baryon-baryon potentials incorporated, exhibit dependence on the strangeness fraction similar to those from Ref. [81].

We now show the results for the pressure. In general, the effect from the isospin asymmetric environment is much stronger than that from strangeness mixing. These results also can be seen from the density dependence of the pressure shown in Fig. 5, where we draw the results for the dependence of the pressure on λ for possible four different cases, as discussed in the case of binding energy dependence on normalized nuclear matter density. One can see that the strangeness mixing will bring about the softening of EoS, comparing the blue solid curve with the green dotted ones or the red dashed and grey dashed ones.

IV. BARYONS MASSES IN DIFFERENT BARYON ENVIRONMENTS

We are now in a position to discuss how the masses of the SU(3) baryons undergo the changes in ordinary and strangeness-mixed nuclear matter. Since all the medium functions have been already fixed, we can study the modification of the baryon masses in different nuclear media. While we have considered only the baryon octet in formulating the nuclear matter, we will investigate the medium modifications of both the baryon octet and decuplet in nuclear matter.

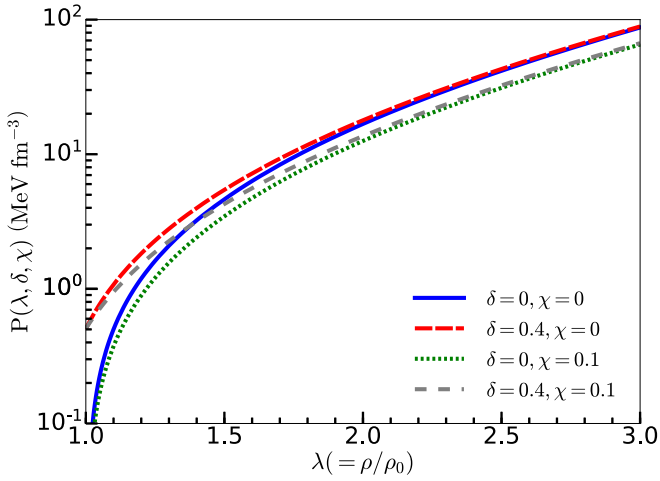

FIG. 5. Pressure $P(\lambda, \delta, \chi)$ as a function of the normalized nuclear matter density $\lambda = \rho/\rho_0$. Notations and parameters are the same as described in the caption of Fig. 4.

The contributions from the surrounding baryon environment can be divided into two parts: the change of the classical soliton mass $\Delta M_{\rm cl} = M^*_{\rm cl} - M_{\rm cl}$ [see Eq. (14)] and that of quantum fluctuations $\Delta M_{\rm qf} = \Delta M_B - \Delta M_{\rm cl}$, where $\Delta M_B = M^*_B - M_B$ denotes the shift in the baryon mass. From the values of the parameters in Eq. (37), one can see that the classical soliton mass is homogeneously dropped in nuclear matter. The soliton mass in free space in the present work is 737.6 MeV. Its change in the medium at the normal nuclear matter density ($\lambda = 1$) is given as -41.38 MeV. In the case of quantum fluctuations the situations is not at all trivial, because different parts of the quantum fluctuations may behave in a different way depending on the content of the surrounding baryon environment.

The masses of octet and decuplet member baryons in the different baryon environments at normal nuclear matter $\lambda = 1$ density are predicted and are listed in Table II. One can see that the change of quantum fluctuations and, consequently, the changes of baryons masses in the different environments are different. In the symmetric ordinary nuclear matter ($\lambda = 1$ and $\delta = 0$) the masses of the baryon octet and decuplet decrease as λ increases (compare third and fourth columns in Table II). Figure 6 illustrates the density dependence of the mass shifts of the nucleon and Δ isobar in the isospin symmetric nuclear matter. As shown in Fig. 6, the mass shift of the nucleon decreases very slowly as λ increases. However, it is almost saturated in the vicinity of the normal nuclear matter density and then starts to increase very slightly. However, the mass shift of the Δ isobar falls off monotonically as λ increases. Since the mass difference of the nucleon and Δ comes from the zero-mode quantization of the chiral soliton, the medium modification of the zero-mode quantum fluctuation for the Δ comes into essential play. This fact makes the mass shift of Δ turn out to be very different from that of the nucleon. We find the very similar results for the other members of the baryon octet and decuplet.

However, the situation is changed in isospin-asymmetric matter. The mass shift of the SU(3) baryons in the isospin asymmetric environment depends on the third component of baryons isospin. Thus, the mass shifts of the baryons are more pronounced, in particular, for the baryon with negative T_3. For example, the mass shift of the proton in pure neutron matter ($\delta = 1$) at normal nuclear matter density ($\lambda = 1$) is obtained to be -48.79 MeV, while that of the neutron becomes positive, i.e., $+15.20$ MeV (see also Table II). This implies that the up and down quarks may undergo changes in a different manner.

The results for the mass shifts of the baryon octet and decuplet in the pure neutron matter are shown in Figs. 7(a) and 7(b), respectively. First of all, one can explicitly see that the

TABLE II. Masses of the baryon octet and decuplet both in free space and in the different baryon environments at normal nuclear matter density $\lambda = 1$. The parameters for the symmetry energy are taken from Set I in Table I. All the masses are given in units of MeV.

Baryon	Exp	Free space	$\delta = 0, \chi = 0$	$\delta = 1, \chi = 0$	$\delta = 0, \chi = 0.1$	$\delta = 0.4, \chi = 0.1$
p	938.76	938.01	921.97	889.97	918.23	905.43
n	940.27	939.52	922.47	955.47	919.73	932.53
Λ	1109.61	1108.86	1092.82	1092.82	1092.77	1092.77
Σ^+	1188.75	1188.00	1171.96	1106.74	1172.01	1145.92
Σ^0	1190.20	1189.45	1173.41	1173.41	1173.46	1173.46
Σ^-	1195.48	1194.73	1178.69	1243.91	1178.74	1204.83
Ξ^0	1319.30	1318.55	1302.51	1269.29	1306.21	1292.92
Ξ^-	1321.31	1323.78	1307.74	1340.96	1311.40	1324.72
Δ^{++}	1230.55	1247.79	1137.60	1041.30	1133.94	1095.42
Δ^+	1234.90	1248.61	1138.42	1106.31	1134.75	1121.91
Δ^0	1231.3	1250.79	1140.59	1172.70	1136.93	1149.77
Δ^-	1230 to 1234	1254.33	1144.14	1240.44	1140.48	1179.00
Σ^{*+}	1382.80	1387.73	1277.54	1213.34	1277.54	1251.86
Σ^{*0}	1383.70	1389.91	1279.72	1279.72	1279.72	1279.72
Σ^{*-}	1394.20	1393.46	1283.27	1374.47	1283.27	1308.95
Ξ^{*0}	1531.80	1529.03	1418.84	1386.74	1422.50	1409.66
Ξ^{*-}	1535.0	1532.58	1422.39	1454.49	1426.05	1438.89
Ω^-	1672.45	1671.70	1561.51	1561.51	1568.84	1568.84

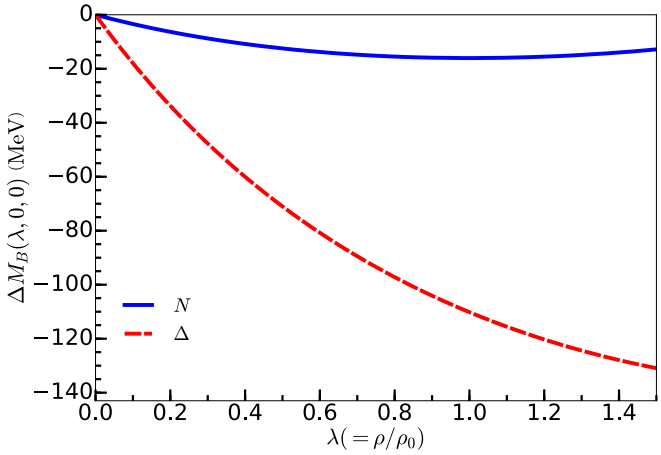

FIG. 6. The result for the mass shift $\Delta M_B = M_B^* - M_B$ of the nucleon $B = N$ in the isospin symmetric nuclear matter is drawn in a solid curve, whereas that of the $B = \Delta$ isobar is depicted in a dashed one.

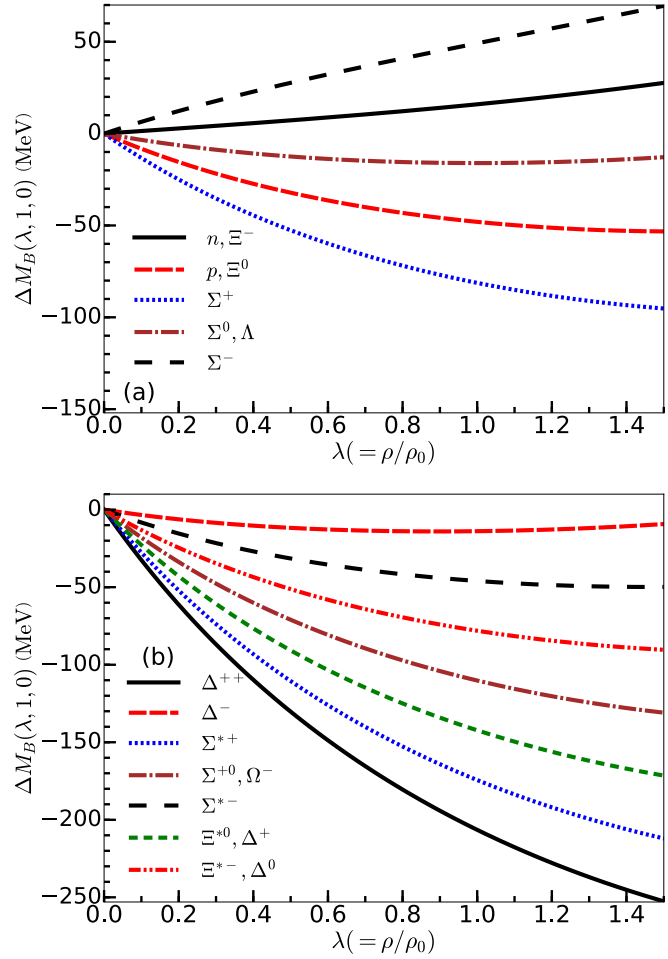

FIG. 7. Results for the mass shifts ΔM_B of the baryon octet and the decuplet in the pure neutron matter ($\delta = 1$) are drawn in panels (a) and (b), respectively. The parameters for the symmetry energy are taken from Set I in Table I.

effects of the isospin mass splitting are clearly shown in the isospin-asymmetric nuclear environment. Depending on the charges of the baryon octet, we can see that their mass shifts behave in a very different way. As shown Fig. 7(a), the neutron mass increases as λ increases, whereas the proton mass drops off as λ increases. In general, the masses of the members in the baryon octet with the negative values of T_3 rises in the neutron matter as λ increases. However, the masses of the octet baryons with the positive values of T_3 drop off as λ decreases. However, while the mass of Ξ^0 is identical to that of the proton, those of Σ^0 and Λ^0, which are also identical to each other, fall off slowly and then are saturated as λ increases. This is originated from the fact that the in-medium functionals for the quantum fluctuations near the third component of isospin are quite sensitive to the medium effects and they are identical for the baryons that have the same isospin components.

The isospin factor in neutron matter was also studied in Ref. [83] based on the low-energy hyperon-nucleon scattering data and on the hypertriton derived from an effective field theory to the next-to-leading order at low densities. In Ref. [83] the Λ mass decreases in both symmetric and asymmetric matters. This behaviors are in qualitative agreement with the present ones. On the contrary, the mass of Σ increases in symmetric matter from Ref. [83] while the present results show opposite tendency, that is, the Σ mass increases as the density increases.

The general tendency and the effects of the isospin factor can be seen also in the case of decuplet baryons, which are given in Fig. 7(b), but the mass shifts are larger than those of the baryon octet. For example, the mass shift in the isospin averaged Δ in normal nuclear matter is around two times smaller than the Δ^{++} mass shift in neutron matter at normal nuclear matter density $\lambda = 1$. For example, one can see this by comparing the red dashed curve in Fig. 6 with the black solid one in Fig. 7(b). The isospin component factor is similar to the octet case and some baryons masses such as Ξ^{*0} and Δ^+ have the identical dependence on λ. Due to the isospin factor, the Δ^- mass in neutron matter remains almost constant which is seen from the red dashed curve in Fig. 7(b). The present results are in qualitative agreement with those from Ref. [84].

The present work shows that the mass shifts are more pronounced in the isospin asymmetric matter in comparison with those in the symmetric matter. Similar results were obtained in a chiral SU(3) quark mean-field model [16]. The mass shifts of hyperons in nuclear matter were also studied in Ref. [85], of which the results are also in qualitative agreement with the present ones.

For completeness, we show also the mass changes of the baryons in the strangeness-mixed asymmetric environment. In Fig. 8, the results for the mass shifts of the nucleon and Δ in strangeness-mixed asymmetric matter are presented as functions of λ, which we choose them as the representatives of the baryon octet and decuplet, respectively. For the sake of the illustration, we include the changes of isospin-averaged masses of the nucleon and Δ by the black solid curves in Figs. 8(a) and 8(b), respectively. Figure 8 explicitly shows the isospin factor in nuclear matter, which are explained above. It also depicts how the strength of the mass are changed due to the environment content. Comparing Figs. 7 and 8, one can

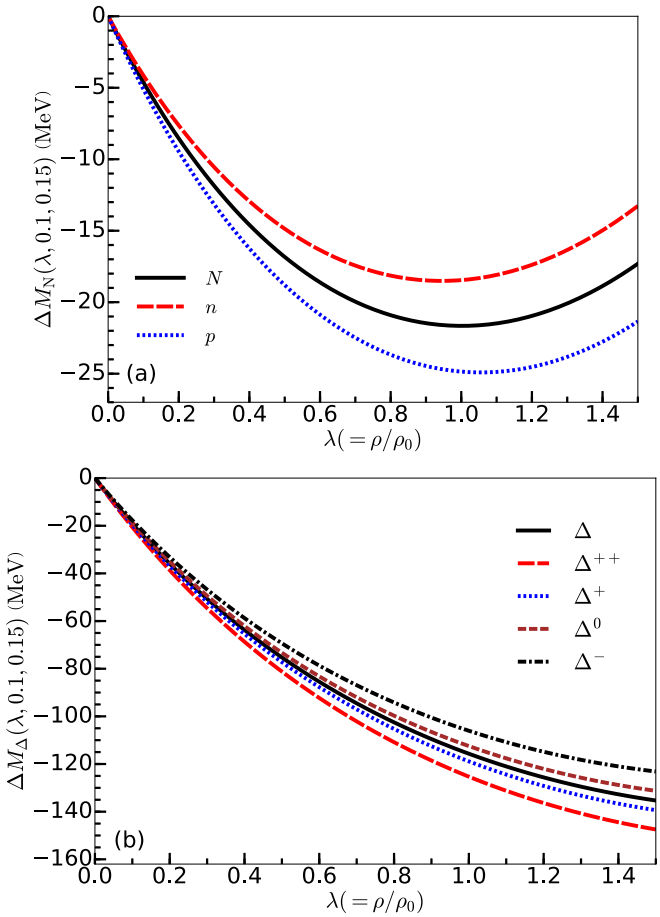

FIG. 8. Mass shifts $M_B^* - M_B$ of the nucleon (a) and Δ isobar (b) in the strangeness mixed isospin-asymmetric matter.

conclude that the changes in neutron matter are stronger than those in strange matter. In general, the results in strangeness-mixed matter are rather similar to those in pure neutron matter.

V. SUMMARY AND OUTLOOK

In the present work, we have investigated the various baryonic matters such as the symmetric nuclear matter, pure neutron matter, and strangeness-mixed baryonic matter, based on the meson mean-field approach or the generalized SU(3) chiral soliton model. All the dynamical parameters for the baryon masses in the model were determined by using the experimental data in free space and then we have introduced the parametrizations for the density-dependent parameters. As a starting point, we took a "*model-independent approach*" for the SU(3) baryon properties in free space, which described successfully the baryon masses of the baryon decuplet and other properties of baryons in free space [23,24]. In the present work, the medium modifications of the model functionals were carried out by employing the linear density-dependent forms. Having determined the parameters for the medium modification by using the empirical data related to nuclear matter such as the binding energy per nucleon, the compressibility, and the symmetry energy, we were able to describe the equation of states for various nuclear environments including the nonstrange sector. We found that the present results were in good agreement with the data extracted from the phenomenology and experiments and with the results from other approaches. We also discussed the properties of the strangeness-mixed matter and they also were in agreement with the phenomenology. Finally, we predicted the mass shifts of the baryon octet and decuplet in various baryonic environments with different content of the isospin asymmetry and strangeness. We scrutinized the changes of the masses of the baryons with different values of the third components of isospin and found that the masses of the baryons with negative charges show very different dependence on the nuclear matter density from those with positive and null charges.

Since we have formulated the equations of states for isospin-asymmetric and strangeness-mixing baryonic matter, one can directly apply the present model to investigate properties of neutron stars. The corresponding investigation is under way.

ACKNOWLEDGMENTS

The present work was supported by Basic Science Research Program through the National Research Foundation of Korea funded by the Korean government (Ministry of Education, Science and Technology, MEST), Grants No. 2019R1A2C1010443 (Gh.-S.Y.), No. 2018R1A2B2001752 and No. 2018R1A5A1025563 (H.-Ch.K.), and No. 2020R1F1A1067876 (U.Y.).

APPENDIX: MASSES OF BARYONS IN FREE SPACE

The masses of baryon octet are expressed as

$$M_N = M_{\rm cl} + E_{(1,1),1/2} + \tfrac{1}{5}\big(c_8 + \tfrac{4}{9}c_{27}\big)T_3 + \tfrac{3}{5}\big(c_8 + \tfrac{2}{27}c_{27}\big)\big(T_3^2 + \tfrac{1}{4}\big) - (d_1 - d_2)T_3 - (D_1 + D_2), \quad \text{(A1)}$$

$$M_\Lambda = M_{\rm cl} + E_{(1,1),1/2} + \tfrac{1}{10}\big(c_8 - \tfrac{2}{3}c_{27}\big) - D_2, \quad \text{(A2)}$$

$$M_\Sigma = M_{\rm cl} + E_{(1,1),1/2} + \tfrac{1}{2}\big(T_3 - \tfrac{1}{5}\big)c_8 + \tfrac{2}{9}\big(T_3^2 - \tfrac{7}{10}\big)c_{27} - \big(d_1 + \tfrac{1}{2}d_2\big)T_3 + D_2, \quad \text{(A3)}$$

$$M_\Xi = M_{\rm cl} + E_{(1,1),1/2} + \tfrac{4}{5}\big(c_8 - \tfrac{1}{9}c_{27}\big)T_3 - \tfrac{2}{5}\big(c_8 - \tfrac{1}{9}c_{27}\big)\big(T_3^2 + \tfrac{1}{4}\big) - (d_1 + 2d_2)T_3 + D_1, \quad \text{(A4)}$$

where $E_{(1,1),1/2}$ can be obtained from Eq. (24). The masses of the baryon decuplet are given by the following expressions:

$$M_\Delta = M_{\rm cl} + E_{(3,0)3/2} + \tfrac{1}{4}\big(c_8 + \tfrac{8}{63}c_{27}\big)T_3 + \tfrac{5}{63}T_3^2 + \tfrac{1}{8}\big(c_8 - \tfrac{2}{3}c_{27}\big) - \big(d_1 - \tfrac{3}{4}d_2\big)T_3 - \big(D_1 - \tfrac{3}{4}D_2\big), \quad \text{(A5)}$$

$$M_{\Sigma^*} = M_{\rm cl} + E_{(3,0),3/2} + \tfrac{1}{4}\big(c_8 - \tfrac{4}{21}c_{27}\big)T_3 + \tfrac{5}{63}c_{27}\big(T_3^2 - 1\big) - \big(d_1 - \tfrac{3}{4}d_2\big)T_3, \quad \text{(A6)}$$

$$M_{\Xi^*} = M_{\rm cl} + E_{(3,0),3/2} + \tfrac{1}{4}\big(c_8 - \tfrac{32}{63}c_{27}\big)T_3 - \tfrac{1}{4}\big(c_8 + \tfrac{8}{63}c_{27}\big)\big(T_3^2 + \tfrac{1}{4}\big) - \big(d_1 - \tfrac{3}{4}d_2\big)T_3 + \big(D_1 - \tfrac{3}{4}D_2\big), \quad \text{(A7)}$$

$$M_{\Omega} = M_{\rm cl} + E_{(3,0),3/2} - \tfrac{1}{4}\big(c_8 - \tfrac{4}{21}c_{27}\big) + 2\big(D_1 - \tfrac{3}{4}D_2\big), \quad \text{(A8)}$$

where $E_{(3,0),3/2}$ can be obtained from Eq. (24). Here $d_{1,2}$ and $D_{1,2}$ are defined as

$$d_1 = (m_d - m_u)\big[-\tfrac{1}{5}\alpha - \beta + \tfrac{1}{5}\gamma\big], \quad \text{(A9)}$$

$$d_2 = (m_d - m_u)\big[-\tfrac{1}{10}\alpha - \tfrac{3}{20}\gamma\big], \quad \text{(A10)}$$

$$D_1 = (m_s - \bar{m})\big[-\tfrac{1}{5}\alpha - \beta + \tfrac{1}{5}\gamma\big], \quad \text{(A11)}$$

$$D_2 = (m_s - \bar{m})\big[-\tfrac{1}{10}\alpha - \tfrac{3}{20}\gamma\big]. \quad \text{(A12)}$$

The explicit forms of c_8 and c_{27}, which denote the wave-function corrections, can be found in Ref. [23].

[1] E. G. Drukarev and E. M. Levin, Prog. Part. Nucl. Phys. **27**, 77 (1991).
[2] M. C. Birse, J. Phys. G **20**, 1537 (1994).
[3] G. E. Brown and M. Rho, Phys. Rep. **269**, 333 (1996).
[4] K. Saito, K. Tsushima, and A. W. Thomas, Prog. Part. Nucl. Phys. **58**, 1 (2007).
[5] B. D. Serot and J. D. Walecka, Adv. Nucl. Phys. **16**, 1 (1986).
[6] J. J. Aubert *et al.* (European Muon Collaboration), Phys. Lett. B **123**, 275 (1983).
[7] S. Strauch *et al.* (Jefferson Lab E93-049 Collaboration), Phys. Rev. Lett. **91**, 052301 (2003).
[8] G. Agakishiev *et al.* (HADES Collaboration), Phys. Rev. C **90**, 054906 (2014).
[9] S. Malace, D. Gaskell, D. W. Higinbotham, and I. Cloet, Int. J. Mod. Phys. E **23**, 1430013 (2014).
[10] K. J. Eskola, P. Paakkinen, H. Paukkunen, and C. A. Salgado, Eur. Phys. J. C **77**, 163 (2017).
[11] T. Kolar *et al.* (A1 Collaboration), Phys. Lett. B **811**, 135903 (2020).
[12] F. Osterfeld, Rev. Mod. Phys. **64**, 491 (1992).
[13] H. Lenske, M. Dhar, T. Gaitanos, and X. Cao, Prog. Part. Nucl. Phys. **98**, 119 (2018).
[14] R. Knorren, M. Prakash, and P. J. Ellis, Phys. Rev. C **52**, 3470 (1995).
[15] P. Papazoglou, S. Schramm, J. Schaffner-Bielich, H. Stocker, and W. Greiner, Phys. Rev. C **57**, 2576 (1998).
[16] P. Wang, Z. Y. Zhang, Y. W. Yu, R. K. Su, and Q. Song, Nucl. Phys. A **688**, 791 (2001).
[17] J. M. Lattimer, Ann. Rev. Nucl. Part. Sci. **62**, 485 (2012).
[18] I. Vidaña, Proc. R. Soc. Lond. A **474**, 0145 (2018).
[19] D. Diakonov, V. Y. Petrov, and P. V. Pobylitsa, Nucl. Phys. B **306**, 809 (1988).
[20] E. Witten, Nucl. Phys. B **160**, 57 (1979).
[21] E. Witten, Nucl. Phys. B **223**, 422 (1983); **223**, 433 (1983).
[22] G. S. Yang, H.-Ch. Kim, and M. V. Polyakov, Phys. Lett. B **695**, 214 (2011).
[23] G. S. Yang and H.-Ch. Kim, Prog. Theor. Phys. **128**, 397 (2012).
[24] G. S. Yang and H.-Ch. Kim, Phys. Rev. C **92**, 035206 (2015).
[25] G. S. Yang, H.-Ch. Kim, M. V. Polyakov, and M. Praszałowicz, Phys. Rev. D **94**, 071502(R) (2016).
[26] H.-Ch. Kim, M. V. Polyakov, and M. Praszałowicz, Phys. Rev. D **96**, 014009 (2017); **96**, 039902(E) (2017).
[27] H.-Ch. Kim, M. V. Polyakov, M. Praszałowicz, and G. S. Yang, Phys. Rev. D **96**, 094021 (2017); **97**, 039901(E) (2018).
[28] G. S. Yang and H.-Ch. Kim, Phys. Lett. B **785**, 434 (2018).
[29] G. S. Yang and H.-Ch. Kim, Phys. Lett. B **781**, 601 (2018).
[30] G. S. Yang and H.-Ch. Kim, Phys. Lett. B **801**, 135142 (2020).
[31] G. S. Yang and H.-Ch. Kim, Phys. Lett. B **808**, 135619 (2020).
[32] C. V. Christov, A. Blotz, H.-Ch. Kim, P. Pobylitsa, T. Watabe, T. Meissner, E. Ruiz Arriola, and K. Goeke, Prog. Part. Nucl. Phys. **37**, 91 (1996).
[33] G. S. Adkins and C. R. Nappi, Nucl. Phys. B **249**, 507 (1985).
[34] J. Berger and C. V. Christov, Nucl. Phys. A **609**, 537 (1996).
[35] A. M. Rakhimov, M. M. Musakhanov, F. C. Khanna, and U. T. Yakhshiev, Phys. Rev. C **58**, 1738 (1998).
[36] U. Yakhshiev and H.-Ch. Kim, Phys. Rev. C **83**, 038203 (2011).
[37] H.-Ch. Kim, P. Schweitzer, and U. Yakhshiev, Phys. Lett. B **718**, 625 (2012).
[38] J. H. Jung, U. Yakhshiev, and H.-Ch. Kim, J. Phys. G **41**, 055107 (2014).
[39] K. H. Hong, U. Yakhshiev, and H.-Ch. Kim, Phys. Rev. C **99**, 035212 (2019).
[40] U. T. Yakhshiev, M. M. Musakhanov, A. M. Rakhimov, U. G. Meissner, and A. Wirzba, Nucl. Phys. A **700**, 403 (2002).
[41] U. T. Yakhshiev, Ulf-G. Meißner, A. Wirzba, A. M. Rakhimov, and M. M. Musakhanov, Phys. Rev. C **71**, 034007 (2005).
[42] U. G. Meissner, A. M. Rakhimov, A. Wirzba, and U. T. Yakhshiev, Eur. Phys. J. A **36**, 37 (2008).
[43] J. H. Jung, U. T. Yakhshiev, and H.-Ch. Kim, Phys. Lett. B **723**, 442 (2013).
[44] U. T. Yakhshiev, Phys. Rev. C **88**, 034318 (2013).
[45] U. Yakhshiev, Phys. Lett. B **749**, 507 (2015).
[46] W. Pauli and S. M. Dancoff, Phys. Rev. **62**, 85 (1942).
[47] T. H. R. Skyrme, Nucl. Phys. **31**, 556 (1962).
[48] D. Diakonov, in *Proceedings of the Advanced School on Nonperturbative Quantum Field Physics*, Peñíscola, Castellón, Spain (1997), pp. 1–55.
[49] E. Guadagnini, Nucl. Phys. B **236**, 35 (1984).
[50] P. O. Mazur, M. A. Nowak, and M. Praszalowicz, Phys. Lett. **147B**, 137 (1984).
[51] S. Jain and S. R. Wadia, Nucl. Phys. B **258**, 713 (1985).
[52] A. Blotz, D. Diakonov, K. Goeke, N. W. Park, V. Petrov, and P. V. Pobylitsa, Nucl. Phys. A **555**, 765 (1993).
[53] A. Blotz, K. Goeke, and M. Praszałowicz, Acta Phys. Polon. B **25**, 1443 (1994).
[54] H. A. Bethe and R. F. Bacher, Rev. Mod. Phys. **8**, 82 (1936).
[55] C. F. V. Weizsacker, Z. Phys. **96**, 461 (1935).
[56] M. M. Sharma, W. T. A. Borghols, S. Brandenburg, S. Crona, A. van der Woude, and M. N. Harakeh, Phys. Rev. C **38**, 2562 (1988).
[57] S. Shlomo and D. H. Youngblood, Phys. Rev. C **47**, 529 (1993).

[58] Z. Ma, N. Van Giai, H. Toki, and M. L'Huillier, Phys. Rev. C **55**, 2385 (1997).
[59] D. Vretenar, T. Niksic, and P. Ring, Phys. Rev. C **68**, 024310 (2003).
[60] B. Ter Haar and R. Malfliet, Phys. Rep. **149**, 207 (1987).
[61] R. Brockmann and R. Machleidt, Phys. Rev. C **42**, 1965 (1990).
[62] J. R. Stone, N. J. Stone, and S. A. Moszkowski, Phys. Rev. C **89**, 044316 (2014).
[63] S. Shlomo, V. M. Kolomietz, and G. Colo, Eur. Phys. J. A **30**, 23 (2006).
[64] E. Chabanat, J. Meyer, P. Bonche, R. Schaeffer, and P. Haensel, Nucl. Phys. A **627**, 710 (1997).
[65] C. B. Das, S. Das Gupta, C. Gale, and B. A. Li, Phys. Rev. C **67**, 034611 (2003).
[66] X. Roca-Maza, X. Viñas, M. Centelles, B. K. Agrawal, G. Colo', N. Paar, J. Piekarewicz, and D. Vretenar, Phys. Rev. C **92**, 064304 (2015).
[67] L. Chen, Sci. China G **52**, 1494 (2009).
[68] A. Akmal, V. R. Pandharipande, and D. G. Ravenhall, Phys. Rev. C **58**, 1804 (1998).
[69] P. Danielewicz and J. Lee, Nucl. Phys. A **922**, 1 (2014).
[70] D. H. Youngblood, H. L. Clark, and Y.-W. Lui, Phys. Rev. Lett. **82**, 691 (1999).
[71] W. G. Lynch, M. B. Tsang, Y. Zhang, P. Danielewicz, M. Famiano, Z. Li, and A. W. Steiner, Prog. Part. Nucl. Phys. **62**, 427 (2009).
[72] P. Danielewicz, R. Lacey, and W. G. Lynch, Science **298**, 1592 (2002).
[73] A. W. Steiner, J. M. Lattimer, and E. F. Brown, Astrophys. J. Lett. **765**, L5 (2013).
[74] M. Dutra, O. Lourenco, S. S. Avancini, B. V. Carlson, A. Delfino, D. P. Menezes, C. Providencia, S. Typel, and J. R. Stone, Phys. Rev. C **90**, 055203 (2014).
[75] C. Fuchs, Prog. Part. Nucl. Phys. **56**, 1 (2006).
[76] M. B. Tsang *et al.*, Phys. Rev. C **86**, 015803 (2012).
[77] S. Gandolfi, J. Carlson, and S. Reddy, Phys. Rev. C **85**, 032801(R) (2012).
[78] A. W. Steiner and S. Gandolfi, Phys. Rev. Lett. **108**, 081102 (2012).
[79] H. J. Schulze, M. Baldo, U. Lombardo, J. Cugnon, and A. Lejeune, Phys. Rev. C **57**, 704 (1998).
[80] H. Lenske and M. Dhar, Lect. Notes Phys. **948**, 161 (2018).
[81] V. G. J. Stoks and T. S. H. Lee, Phys. Rev. C **60**, 024006 (1999).
[82] J. Schaffner-Bielich and A. Gal, Phys. Rev. C **62**, 034311 (2000).
[83] C. L. Korpa, A. E. L. Dieperink, and R. G. E. Timmermans, Phys. Rev. C **65**, 015208 (2001).
[84] M. J. Savage and M. B. Wise, Phys. Rev. D **53**, 349 (1996).
[85] K. Saito and A. W. Thomas, Phys. Rev. C **51**, 2757 (1995).